shown to conversely relate with HSC activity in fetal liver.[26] Lin$^-$ c-kit^{Hi} Sca1$^+$ cells could be divided into ESAM$^-$ and ESAM$^+$ fractions, and a subpopulation with higher Sca1 expression was more enriched with ESAM$^+$ cells (Figure 2C, middle and right). CD48 expression tended to increase along with down-regulation of ESAM. Indeed, the Lin$^-$ c-kit^{Hi} Sca1$^+$ fraction was found to consist of two major subpopulations, CD48^{Hi} ESAM$^-$ and CD48$^{-/Lo}$ ESAM$^+$. Thus, ESAM is conspicuously expressed on immature hematopoietic cells in fetal liver, and seems to conversely relate to lineage progression.

ESAM expression is closely associated with fetal HSC among endothelial markers.

Next we evaluated how ESAM corresponds to other endothelial antigens that were previously identified on fetal hematopoietic progenitors. CD34 and CD31/PECAM1 were uniformly present on Rag1$^-$ c-kit^{Hi} Sca1$^+$ cells in E14.5 fetal liver (Figure 3A and 3B). Neither could resolve the Rag1$^-$ c-kit^{Hi} Sca1$^+$ cells into ESAM^{Hi} and ESAM$^{-/Lo}$ fractions, and even showed a slightly inverse relationship with ESAM expression on early progenitors. Expression profiles of Endoglin and Tie2 did correlate with ESAM (Figure 3C and 3D). However, while the primitive ESAM^{Hi} fraction uniformly expressed high levels of Endoglin and Tie2, many of the more differentiated ESAM$^{-/Lo}$ cells still retained the two markers. These results suggested that ESAM might be a more useful marker of HSC than other endothelial antigens, and could represent an important tool for fetal stem cell studies.

ESAM is useful to enrich primitive multipotent progenitors from fetal liver.

To evaluate whether ESAM expression can enrich primitive progenitors in fetuses, we compared the clonogenic potential in methylcellulose cultures of the ESAM$^{-/Lo}$ and ESAM^{Hi} cells in the Rag1$^-$ ckit^{Hi} Sca1$^+$ HSC fraction of E14.5 fetal liver. Cells in the ESAM^{Hi} fraction formed more colonies with larger size than those in the ESAM$^{-/Lo}$ fraction (Figure 4A and 4B). In particular, most CFU-Mix, primitive progenitors with both myeloid and erythroid potential, were found in the ESAM^{Hi} fraction (Figure 4A).

Next we analyzed the lymphopoietic potential of cells resolved on the

basis of ESAM in co-cultures with the MS5 bone marrow stromal cell line. The culture media contained SCF, Flt3-L, and IL-7, factors that effectively generate $CD19^+$ B lymphoid cells as well as $Mac1^+$ myeloid cells.[18] When 500 cells were cultured in individual wells of 6-well plates, both $ESAM^{-/Lo}$ and $ESAM^{Hi}$ fractions produced $CD19^+$ cells and $Mac1^+$ cells (Figure 5A). However, we observed that most of the hematopoietic colonies from $ESAM^{Hi}$ cells grew beneath the MS5 stromal cell layer, while this was not the case with $ESAM^{-/Lo}$ cells (data not shown). Moreover, the lympho-hematopoietic cells from $ESAM^{Hi}$ cells continued to expand explosively after 6 days of co-culture and gave rise to approximately 50,000 cells per input progenitor by day 10 (Figure 5B).

Authentic HSC are characterized as having both lymphoid and myeloid potential.[8,27] To compare numbers of primitive lympho-hematopoietic progenitors in the $ESAM^{Hi}$ and $ESAM^{-/Lo}$ fractions, we performed in vitro limiting dilution assays in MS5 co-cultures. One in 2.1 $ESAM^{Hi}$ cells and 1 in 3.5 $ESAM^{-/Lo}$ cells gave rise to blood cells, indicating that both fractions are extremely potent sources of hematopoietic progenitors (Figure 5C left). However, we observed drastic differences between the two regarding the frequencies of primitive progenitors with lymphopoietic potential. While 1 in 8 $ESAM^{Hi}$ cells produced $CD19^+$ B lineage cells, only 1 in 125 $ESAM^{-/Lo}$ cells were lymphopoietic under these conditions (Figure 5C right). These results suggest that primitive stem/progenitor cells, which are multipotent for myeloid, erythroid, and lymphoid lineages, are present in the $ESAM^{Hi}$ fraction of fetal liver.

Long-term reconstitution activity is exclusive to $ESAM^{Hi}$ cells.

To evaluate ESAM expression on long-term reconstituting HSC in E14.5 fetal liver, we transplanted cells of the $ESAM^{-/Lo}$ or $ESAM^{Hi}$ fraction into lethally irradiated mice (Figure 6A). Five weeks after transplantation, it was obvious that $CD45.2^+$ $ESAM^{Hi}$ cells contributed highly to the recovery of hematopoiesis in recipients, but no chimerism was detected in mice transplanted with $ESAM^{-/Lo}$ cells (Figure 6B). Indeed, although 9 out of 11 mice transplanted with 1,000 $ESAM^{Hi}$ cells had clear donor $CD45.2^+$ populations (>1.0%) among peripheral leukocytes, none of 10 mice given 1,000 $ESAM^{-/Lo}$ cells had evidence of chimerism. Five months after transplantation, we analyzed the contribution

of CD45.2$^+$ cells to long-term lympho-hematopoietic reconstitution of the recipients. While most of the 11 mice transplanted with ESAM^{Hi} cells had clear CD45.2$^+$ populations in bone marrow (mean ± SD of % CD45.2$^+$ CD45.1$^-$ in total CD45$^+$ cells; 16.3 ± 22.0%), none of the ESAM$^{-/Lo}$-transplanted mice contained detectable CD45.2$^+$ cells in that organ (mean ± SD of % CD45.2$^+$ CD45.1$^-$ in total CD45$^+$ cells; 0.02 ± 0.03%) (Figure 6C). Furthermore, multi-lineage recovery was observed in the bone marrow, spleen and thymus of mice transplanted with ESAM^{Hi} cells (Figure 6D). In addition, bone marrow cells recovered from primary recipients with ESAM^{Hi} cell-transplantation effectively reconstituted CD45.2$^+$ lympho-hematopoietic cells in secondary recipients at 5 months after transplantation (data not shown). These results indicate that high levels of ESAM expression correspond to fetal HSC with long-term repopulating potential.

ESAM expression marks cells thought to represent HSC in fetal and aged adult tissues.

The definitive HSC that account for lympho-hematopoieisis in adults first arise in the AGM region.[28,29] To examine whether ESAM was present on those HSC, flow cytometry analyses were performed with the Rag1/GFP$^-$ cells isolated from E10.5 embryos. Tie2 and c-kit were used as additional parameters because we previously identified lympho-hematopoietic cells in the early embryos as Rag1$^-$ Tie2$^+$ c-kit$^+$.[19] A small but conspicuous Tie2^{Hi} population was detected in E10.5 AGM cells (Figure 7A left). Interestingly, the Tie2^{Hi} AGM cells were clearly divided into two discrete populations according to ESAM expression (Figure 7A middle). When the two populations were back-plotted on the Tie2 and c-kit profile, ESAM$^+$ cells were exclusively c-kit$^+$ (Figure 7A right). In addition, lympho-hematopoietic potential in the MS5 co-cultures was highly enriched in the ESAM$^+$ fraction among the Tie2^{Hi} cells. That is, the Tie2^{Hi} ESAM$^+$ fraction could effectively produce both CD19$^+$ lymphoid cells and Mac1$^+$ myeloid cells while the Tie2^{Hi} ESAM$^-$ fraction generated only a small number of Mac1$^+$ cells (Figure 7B). We concluded from these analyses that ESAM marks the primitive hematopoietic cells endowed with lymphopoietic activity in the E10.5 AGM as well as in the E14.5 liver.

A small number of Tie2^{Hi} c-kit^{Lo} ESAM^{Hi} cells were also observed among extraembryonic YS cells (Figure 7C). In addition, the E10.5 YS contained a conspicuous population whose phenotype was Tie2^{Lo} c-kit^{Hi} and cells in that fraction expressed low levels of ESAM (Figure 7C). Cells with the same phenotype were also clearly observed in the E9.5 YS while they were absent in the caudal half of the embryo proper (Supplemental Figure 2A). These Tie2^{Lo} c-kit^{Hi} ESAM^{Lo} cells in the YS effectively produced myeloid and/or erythroid colonies in methylcellulose culture, but showed little lymphopoietic potential (Supplemental Figure 2B and 2C). Importantly, lymphopoietic activity was exclusive to the Tie2^{Hi} c-kit^{Lo} ESAM^{Hi} fraction of the PSp/AGM region, which showed no myeloid-erythroid potential in conventional methylcellulose assays.

It is well known that HSC properties change with developmental age. Indeed, Forsberg et al previously reported ESAM expression by adult marrow HSC [30], but the levels were weak as compared to those on fetal HSC. Therefore, we expected that ESAM, like the other endothelial antigens, would decline with HSC aging. However, we found that ESAM expression was detectable on the Rag1^{-} LSK fraction of bone marrow through life (Figure 7D). Indeed, the proportion of ESAM^{Hi} cells and the mean fluorescence intensity of ESAM expression in the Rag1^{-} LSK fraction increased with age (Figure 7D). Moreover, primitive myeloid-erythroid progenitors from adult bone marrow were also enriched in the ESAM^{Hi} fraction (Figure 7E). In summary, these findings demonstrate that ESAM expression is useful for exploring the biology of hematopoietic stem/progenitor cells throughout life in mice.

Discussion

We conducted gene array analyses with the principal goal of learning more about the initial differentiation of fetal HSC to cells in lymphoid lineages. In that regard, several informative genes were identified and will be presented elsewhere (manuscript in preparation). Our screen also identified genes whose expression was previously thought to correlate with HSC in fetal or adult tissues. Among those, ESAM was particularly noteworthy as being drastically down-regulated during differentiation of HSC to ELP. We now report that it represents a potent tool for identifying HSC over a wide range of developmental age.

ESAM was originally identified as an endothelial cell-specific protein, while it was also shown to be expressed on megakaryocytes and platelets.[22,31] A recent study also found ESAM transcripts in adult marrow HSC when gene arrays were used to compare Thy1.1^{Lo} Flk2^{-} LSK (long-term HSC enriched), Thy1.1^{Lo} Flk2^{+} LSK (short-term HSC) and Thy1.1^{-} Flk2^{+} LSK (multiple progenitors).[30] We now show how ESAM levels can be exploited to obtain highly enriched CFU-Mix, lymphopoietic cells, and long-term HSC from the Rag1^{-} c-kit^{Hi} Sca1^{+} fraction of E14.5 fetal liver. It is important to note that long-term HSC in mouse embryos are unique in expressing markers such as Flk2 and CD11b/Mac1 not characteristic of adult HSC.[18,32] This complicates cell sorting strategies and fetal/adult comparison. We previously found that Rag1/GFP^{-} c-kit^{Hi} Sca1^{+} cells derived from E14.5 fetal liver reconstituted lympho-hematopoiesis in lethally irradiated adults, while Rag1/GFP^{Lo} c-kit^{Hi} Sca1^{+} cells transiently contributed to T and B lymphopoiesis. ESAM specific Abs can be used without knock-in reporters and with fewer combinations of Abs to obtain highly enriched HSC.

Although we identified ESAM as one of the highly expressed genes in HSC but not in ELP, levels of this antigen strongly correlated with lymphopoietic activity. The ESAM^{Hi} fraction in Rag1^{-} c-kit^{Hi} Sca1^{+} cells of E14.5 fetal liver produced CD19^{+} B-lineage cells more effectively and contained lymphopoietic progenitors with even higher frequency than the ESAM$^{-/Lo}$ fraction. The cells also gave rise to long-term reconstitution in both T and B lymphoid lineages in lethally irradiated recipients. Furthermore, in the PSp/AGM region, B

lymphopoietic activity in culture was exclusive to the ESAM^{Hi} Tie2^{+} fraction. From these observations, we conclude that ESAM expression indicates high lymphopoietic potential in HSC of the fetal liver and hematopoietic cells arising in the AGM region. On the other hand, we presume from the sharp down-regulation in ELP that ESAM is not necessary for early lymphoid differentiation.

We previously reported that the first lymphopoietic cells arise in a Tie2^{+} c-kit^{+} CD34$^{-/Lo}$ CD41^{-} subset in the E8.5 PSp region.[19] In this report we showed clear ESAM expression on lymphopoietic cells contained in a Tie2^{Hi} c-kit^{+} subset of the E9.5-10.5 PSp/AGM. Lymphopoietic activity in early embryos is thought to associate closely with HSC development. Since the first HSC have few reliable surface markers, high ESAM expression must be useful to monitor how the first HSC are developing and moving to other sites. As an additional finding, we detected high myeloid-erythroid but little lymphopoietic potential in a Tie2^{Lo} ckit^{Hi} subset of the YS, whose expression level of ESAM was apparently low. We presume that ESAM^{Hi} Tie2^{Hi} c-kit^{+} cells in the PSp/AGM and ESAM^{Lo} Tie2^{Lo} c-kit^{Hi} cells in the YS differ in their origins and/or as development progresses. If combined with those cell surface markers, a newly described method to trace runt-related transcription factor 1-expressing cells would address several important issues related to "primitive" and "definitive" hematopoiesis.[33]

It is interesting to speculate that ESAM might be important for HSC functions. A previous study showed that ESAM mediates homophilic interactions between endothelial cells [22], and endothelial cells must represent an important component of HSC supportive niches in bone marrow.[34] A subsequent study of ESAM-deficient mice showed impaired migration of neutrophils through vascular walls after normal adhesion.[35] In addition, platelets from ESAM-deficient mice were less prone to disaggregation.[36] Thus, ESAM expressed by endothelial and/or stem cells could have functions associated with HSC adhesion and/or migration.

Osteoblastic stromal cells that line trabecular bone are thought to construct niches containing molecules needed to regulate HSC quiescence, proliferation and differentiation in adult bone marrow.[37,38] Other findings indicate that HSC also interact with sinusoidal endothelial cells at some distance from

bones.[39,40] Osteoblastic and vascular niches are likely to function in complementary ways.[41,42] The fetal liver has no osteoblasts, and HSC niches have not been identified in that site. High level ESAM display suggests it should be further explored within the context of endothelial-HSC interactions.

It was an unexpected but intriguing finding that ESAM levels correlate with the stem cell rich fraction even in 22 months old mice. While many endothelial antigens on HSC decline with aging, Endomucin and Endothelial protein C receptor (CD201) have been reported to be adult HSC markers.[17,43] In humans, angiotensin-converting enzyme (CD143) was recently found to mark HSC through embryonic and adult life.[44] However, ESAM seems unique in actually increasing with aging. Many genes involved in NO-mediated signal transduction, stress responses and inflammation have been linked to HSC aging.[4] P-selectin is one of the most highly up-regulated of those stress-related genes. Of particular interest, P-selectin mediates some leukocyte-vascular endothelium interactions and leukocyte extravasation, functions also attributed to ESAM on neutrophils.[35] Recent reports showed that stem/progenitor cells continuously circulate outside bone marrow and can actively participate in innate immune responses.[45,46] Furthermore, platelets can use P-selectin to recruit marrow hematopoietic cells into sites of injury.[47] Although direct evidence is lacking at this moment, further study might implicate elevated ESAM levels in extra-medullary migration of HSC.

Efficient HSC-based therapies and the emerging field of regenerative medicine will benefit from learning more about what defines stem cells. While patterns of expression of transcription factors and other intracellular proteins are informative, surface markers such as ESAM that are unique to HSC have special utility.

Acknowledgments

We thank Drs N. Sakaguchi (Kumamoto University) and H. Igarashi (Kawasaki Medical School) for the Rag1/GFP knock-in mice.

Authorships

Contribution: T.Y. conducted experiments and analyzed results; T.Y., K.O. P.W.K. and Y.K. designed the research plan and wrote the paper; S.B. and D.W. prepared anti-ESAM Abs; K.K. and T.M. performed and analyzed microarrays.

Conflict-of-interest disclosure: The authors declare no competing financial interests.

Correspondence: Takafumi Yokota, Department of Hematology and Oncology, Osaka University Graduate School of Medicine, C9, 2-2 Yamadaoka, Suita, Osaka 565-0871, Japan; e-mail: yokotat@bldon.med.osaka-u.ac.jp

References

1. Osawa M, Hanada K, Hamada H, Nakauchi H. Long-term lymphohematopoietic reconstitution by a single CD34-low/negative hematopoietic stem cell. Science. 1996;273:242-245.

2. Spangrude GJ, Brooks DM. Mouse strain variability in the expression of the hematopoietic stem cell antigen Ly-6A/E by bone marrow cells. Blood. 1993;82:3327-32.

3. Ogawa M. Changing phenotypes of hematopoietic stem cells. Exp Hematol. 2002;30:3-6.

4. Chambers SM, Shaw CA, Gatza C, Fisk CJ, Donehower LA, Goodell MA. Aging hematopoietic stem cells decline in function and exhibit epigenetic dysregulation. PLoS Biol. 2007;5(8):e201.

5. Yilmaz OH, Kiel MJ, Morrison SJ. SLAM family markers are conserved among hematopoietic stem cells from old and reconstituted mice and markedly increase their purity. Blood. 2006;107:924-930.

6. Takahashi K, Tanabe K, Ohnuki M, et al. Induction of pluripotent stem cells from adult human fibroblasts by defined factors. Cell. 2007;131:861-872.

7. Hanna J, Wernig M, Markoulaki S, et al. Treatment of sickle cell anemia mouse model with iPS cells generated from autologous skin. Science. 2007;318:1920-1923.

8. Nishikawa SI, Nishikawa S, Kawamoto H, et al. In vitro generation of lymphohematopoietic cells from endothelial cells purified from murine embryos. Immunity. 1998;8:761-769.

9. Oberlin E, Tavian M, Blazsek I, Péault B. Blood-forming potential of vascular endothelium in the human embryo. Development. 2002;129:4147-4157.

10. Yoder MC, Hiatt K, Dutt P, Mukherjee P, Bodine DM, Orlic D. Characterization of definitive lymphohematopoietic stem cells in the day 9 murine yolk sac. Immunity. 1997;7:335-344.

11. Takakura N, Huang XL, Naruse T, et al. Critical role of the TIE2 endothelial cell receptor in the development of definitive hematopoiesis. Immunity. 1998;9:677-686.

12. Cho SK, Bourdeau A, Letarte M, Zúñiga-Pflücker JC. Expression and function of CD105 during the onset of hematopoiesis from Flk1(+) precursors. Blood. 2001;98:3635-3642.

13. Matsuoka S, Ebihara Y, Xu M, et al. CD34 expression on long-term repopulating hematopoietic stem cells changes during developmental stages. Blood. 2001; 97:419-425.

14. Sato T, Laver JH, Ogawa M. Reversible expression of CD34 by murine hematopoietic stem cells. Blood. 1999;94:2548-2554.

15. Tajima F, Sato T, Laver JH, Ogawa M. CD34 expression by murine hematopoietic stem cells mobilized by granulocyte colony-stimulating factor. Blood. 2000;96:1989-1993.

16. Randall TD, Weissman IL. Phenotypic and functional changes induced at the clonal level in hematopoietic stem cells after 5-fluorouracil treatment. Blood. 1997;89:3596-3606.

17. Matsubara A, Iwama A, Yamazaki S, et al. Endomucin, a CD34-like sialomucin, marks hematopoietic stem cells throughout development. J Exp Med. 2005 ;202:1483-1492.

18. Yokota T, Kouro T, Hirose J, et al. Unique properties of fetal lymphoid

progenitors identified according to RAG1 gene expression. Immunity. 2003;19:365-375.

19. Yokota T, Huang J, Tavian M, et al. Tracing the first waves of lymphopoiesis in mice. Development. 2006;133:2041-2051.

20. Kuwata N, Igarashi H, Ohmura T, Aizawa S, Sakaguchi N. Cutting edge: absence of expression of RAG1 in peritoneal B-1 cells detected by knocking into RAG1 locus with green fluorescent protein gene. J Immunol. 2001;163:6355-6359.

21. Igarashi H, Gregory SC, Yokota T, Sakaguchi N, Kincade PW. Transcription from the RAG1 locus marks the earliest lymphocyte progenitors in bone marrow. Immunity. 2002;17:117-130.

22. Nasdala I, Wolburg-Buchholz K, Wolburg H, et al. A transmembrane tight junction protein selectively expressed on endothelial cells and platelets. J Biol Chem. 2002; 277:16294-16303.

23. Yuasa H, Oike Y, Iwama A, et al. Oncogenic transcription factor Evi1 regulates hematopoietic stem cell proliferation through GATA-2 expression. EMBO J. 2005;24:1976-1987.

24. Mikkola HK, Fujiwara Y, Schlaeger TM, Traver D, Orkin SH. Expression of CD41 marks the initiation of definitive hematopoiesis in the mouse embryo. Blood. 2003;101:508-516.

25. Akashi K, Traver D, Miyamoto T, Weissman IL. A clonogenic common myeloid progenitor that gives rise to all myeloid lineages. Nature. 2000;404:193-197.

26. Kim I, He S, Yilmaz OH, Kiel MJ, Morrison SJ. Enhanced purification of fetal liver hematopoietic stem cells using SLAM family receptors. Blood.

2006;108:737-744.

27. Cumano A, Dieterlen-Lievre F, Godin I. Lymphoid potential, probed before circulation in mouse, is restricted to caudal intraembryonic splanchnopleura. Cell. 1996;86:907-916.

28. Medvinsky A, Dzierzak E. Definitive hematopoiesis is autonomously initiated by the AGM region. Cell. 1996;86:897-906.

29. de Bruijn MF, Ma X, Robin C, Ottersbach K, Sanchez MJ, Dzierzak E. Hematopoietic stem cells localize to the endothelial cell layer in the midgestation mouse aorta. Immunity. 2002;16:673-683.

30. Forsberg EC, Prohaska SS, Katzman S, Heffner GC, Stuart JM, Weissman IL. Differential expression of novel potential regulators in hematopoietic stem cells. PLoS Genet. 2005;1(3):e28.

31. Hirata Ki, Ishida T, Penta K, et al. Cloning of an immunoglobulin family adhesion molecule selectively expressed by endothelial cells. J Biol Chem. 2001;276:16223-16231.

32. Kincade PW, Owen JJ, Igarashi H, Kouro T, Yokota T, Rossi MI. Nature or nurture? Steady-state lymphocyte formation in adults does not recapitulate ontogeny. Immunol Rev. 2002;187:116-25.

33. Samokhvalov IM, Samokhvalova NI, Nishikawa SI. Cell tracing shows the contribution of the yolk sac to adult haematopoiesis. Nature. 2007;446:1056-1061.

34. Yao L, Yokota T, Xia L, Kincade PW, McEver RP. Bone marrow dysfunction in mice lacking the cytokine receptor gp130 in endothelial cells. Blood. 2005;106:4093-101.

35. Wegmann F, Petri B, Khandoga AG, et al. ESAM supports neutrophil extravasation, activation of Rho, and VEGF-induced vascular permeability. J Exp Med. 2006; 203:1671-1677.

36. Brass LF, Zhu L, Stalker TJ. Novel therapeutic targets at the platelet vascular interface. Arterioscler Thromb Vasc Biol. 2008;28:s43-50.

37. Zhang J, Niu C, Ye L, et al. Identification of the haematopoietic stem cell niche and control of the niche size. Nature. 2003;425:836-841.

38. Calvi LM, Adams GB, Weibrecht KW, et al. Osteoblastic cells regulate the haematopoietic stem cell niche. Nature. 2003;425:841-846.

39. Kiel MJ, Yilmaz OH, Iwashita T, Yilmaz OH, Terhorst C, Morrison SJ. SLAM family receptors distinguish hematopoietic stem and progenitor cells and reveal endothelial niches for stem cells. Cell. 2005;121:1109-1121.

40. Sugiyama T, Kohara H, Noda M, Nagasawa T. Maintenance of the hematopoietic stem cell pool by CXCL12-CXCR4 chemokine signaling in bone marrow stromal cell niches. Immunity. 2006;25:977-988.

41. Yin T, Li L. The stem cell niches in bone. J Clin Invest. 2006;116:1195-1201.

42. Orford KW, Scadden DT. Deconstructing stem cell self-renewal: genetic insights into cell-cycle regulation. Nat Rev Genet. 2008;9:115-128.

43. Balazs AB, Fabian AJ, Esmon CT, Mulligan RC. Endothelial protein C receptor (CD201) explicitly identifies hematopoietic stem cells in murine bone marrow. Blood. 2006;107:2317-2321.

44. Jokubaitis VJ, Sinka L, Driessen R, et al. Angiotensin-converting enzyme (CD143) marks hematopoietic stem cells in human embryonic, fetal, and adult hematopoietic tissues. Blood. 2008;111:4055-4063.

45. Massberg S, Schaerli P, Knezevic-Maramica I, et al. Immunosurveillance by hematopoietic progenitor cells trafficking through blood, lymph, and peripheral tissues. Cell. 2007;131:994-1008.

46. Welner RS, Kincade PW. Stem cells on patrol. Cell. 2007;131:842-4.

47. Massberg S, Konrad I, Schürzinger K, et al. Platelets secrete stromal cell-derived factor 1alpha and recruit bone marrow-derived progenitor cells to arterial thrombi in vivo. J Exp Med. 2006;203:1221-1233.

Figure legends

Figure 1. **ESAM gene is preferentially expressed in the HSC fraction of E14.5 fetal liver.**

Microarray analyses comparing HSC-enriched and ELP-enriched populations were performed. Two independent tests depicted the ESAM gene as preferentially expressed in the HSC-enriched population. Results are shown as relative expression levels of each gene comparing with that of Gapdh of which value is 100. Ratio was calculated by [HSC level]/[ELP level] in each gene. The relative expression levels of c-kit were also shown as internal quality controls.

Figure 2. **Specific expression of ESAM on HSC-enriched fraction of E14.5 fetal liver.**

Flow cytometry analysis was performed for Rag1/GFP$^-$ cells of E14.5 fetal liver using anti-c-kit, anti-Sca1, and anti-ESAM Abs. Firstly Rag1/GFP$^-$ cells were sorted from E14.5 fetal liver of Rag1/GFP knock-in heterozygous fetuses with high purity. The sorted cells were incubated with a purified rat anti-mouse ESAM Ab (1G8) followed by goat anti-rat IgG-FITC. The cells were then stained with anti-c-kit-APC, anti-Sca1-PE, and 7AAD. To minimize the nonspecific binding of anti-c-kit and Sca1 mAbs to the cells wearing goat anti-rat IgG-FITC, the cells were incubated with a rat anti-mouse FcRII/III Ab prior to the anti-c-kit and Sca1 staining. (A) The Rag1/GFP$^-$ cells were analyzed with respect to expression of ESAM, c-kit and Sca1 (Left, middle). Expression of c-kit in the Sca1^{Hi} ESAM^{Hi} cells (middle, inset) is presented (right). (B) The conventional c-kit^{Hi} Sca1$^+$ fraction (left, inset) could be divided into two fractions, ESAM$^{-/Lo}$ and ESAM^{Hi} (middle). The cells were stained with an isotype control IgG (dashed line) or with the anti-ESAM Ab (solid line). The ESAM^{Hi} cells (yellow) were found as c-kit^{Hi} Sca1^{Hi} while the ESAM$^{-/Lo}$ cells (pink) were c-kit^{Hi} Sca1^{Lo} (right). (C) Six-color flow cytometry analysis using an anti-ESAM Ab followed by goat anti-rat IgG-FITC, a PE-anti-CD48 Ab, biotin-anti-lineage marker Abs (TER119, Gr1, CD3, CD45R/B220) followed by SA-PETR, a PE-Cy7-anti-Sca1 Ab, an APC-anti-c-kit and 7AAD was performed for E14.5 fetal liver cells of WT C57B6 embryos. The profile of Lin$^-$ cells regarding c-kit

and Sca1 expression is shown in the left. The Lin$^-$ c-kit^{Hi} Sca1^{Lo} and Lin- c-kit^{Hi} Sca1^{Hi} fractions gated in the left panel were analyzed with respect to expression of ESAM and CD48 (middle and right). The percentage of cells in each gate is indicated in each panel.

Figure 3. **Expression of ESAM and other endothelial antigens on fetal liver HSC fraction.**

The expression pattern of ESAM on Rag1/GFP$^-$ c-kit^{Hi} Sca1$^+$ cells of E14.5 fetal liver was compared with other endothelial cell-related antigens, CD34 (A), CD31/PECAM1 (B), Endoglin (C) and Tie2 (D). The percentage of cells in subpopulation is shown. In the histograms, the staining patterns of ESAM$^{-/Lo}$ cells are shown with dashed lines while those of ESAM^{Hi} cells are tinted and shown with solid lines.

Figure 4. **ESAM expression correlates with CFU activity.**

ESAM$^{-/Lo}$ or ESAM^{Hi} cells of the Rag1/GFP$^-$ ckit^{Hi} Sca1$^+$ fraction of E14.5 fetal liver were sorted and subjected to methylcellulose colony formation assay. Numbers of CFUs (A) and morphology of the colonies derived from the indicated CFUs (B) are shown. The results in (A) are shown as means ± SD. A black bar under (B) shows 500mm. The data are from one of three independent experiments that gave similar results. Significant difference between the two population is indicated (** $p<0.01$).

Figure 5. **ESAM expression enriches primitive progenitors endowed with lymphopoietic activity.**

(A, B) Five hundred of ESAM$^{-/Lo}$ or ESAM^{Hi} cells of the Rag1/GFP$^-$ ckit^{Hi} Sca1$^+$ fraction of E14.5 fetal liver were cultured with MS5 stromal cells in the presence of SCF, Flt3-igand, and IL7. At the indicated period, recovered cells were counted and subjected to flow cytometry (A). Yields of total cells, CD19$^+$ Mac1$^-$ B-lineage cells, and Mac1$^+$ CD19$^-$ myeloid-lineage cells per one input ESAM$^{-/Lo}$ or ESAM^{Hi} progenitor were calculated and given as averages with SD bars (B). (C) Limiting dilution analyses were performed in the MS5 co-culture system to determine the frequency of hematopoietic progenitors (left) and that of

progenitors endowed with lymphopoietic potential (right).

Figure 6. **Long-term hematopoiesis-reconstituting activity is excusive to ESAM^{Hi} fraction.**
(A) The Rag1/GFP$^-$ Sca1$^+$ c-kit^{Hi} cells (CD45.2$^+$) of E14.5 fetal liver were sorted into two fractions, ESAM$^{-/Lo}$ and ESAM^{Hi}. Then, 1000 cells of each fraction were mixed with 2 x 10^5 CD45.1$^+$ whole adult bone marrow cells of 10 weeks old mice, and transplanted to a lethally irradiated CD45.1 mouse (A). (B) Flow cytmetry analyses for peripheral leukocytes were performed at 5 weeks after transplantation. In the two independent experiments, 9 out of 11 recipients with ESAM^{Hi} cells were clearly reconstituted by CD45.2$^+$ cells (>1.0% in all of myeloid, T and B lineages) while none of 11 recipients with ESAM$^{-/Lo}$ cells had CD45.2$^+$ cells detectable in the flow cytometry. The figure shows representative results in each group. (C, D) Twenty weeks after transplantation, all the recipients were killed and the contribution of CD45.2$^+$ ESAM^{Hi} cells was evaluated in lympho-hematopoietic organs. Percentages of CD45.2$^+$ CD45.1$^-$ population among total CD45$^+$ cells in bone marrow of each recipient were plotted (C). The long-term re-constitution of CD45.2$^+$ ESAM^{Hi} cells was confirmed with respect to myeloid, B lymphoid, or T lymphoid lineages in the bone marrow, spleen and thymus, respectively (D).

Figure 7. **ESAM marks early hematopoietic progenitors throughout life.**
(A) Rag1/GFP$^-$ cells were sorted from AGM of E10.5 Rag1/GFP knock-in heterozygous fetuses with high purity. The sorted Rag1/GFP$^-$ cells were incubated with the anti-ESAM Ab (1G8) followed by goat anti-rat IgG-FITC. The cells were then stained with anti-c-kit-APC, anti-Tie2-PE, and 7AAD. The profile of Tie2 and c-kit expression in AGM cells was shown in a left panel. ESAM expression (solid line) in the Tie2^{Hi} fraction of AGM and its control level with an isotype matched IgG (dashed line) are presented (middle). The Tie2^{Hi} ESAM$^+$ cells (yellow) were c-kit$^+$ while the Tie2^{Hi} ESAM$^-$ cells (pink) were c-kit$^-$ (right). (B) The Tie2^{Hi} ESAM$^-$ and Tie2^{Hi} ESAM$^+$ cells were sorted from E10.5 AGM and cultured on MS5 for 10 days. The recovered cells were counted and stained for the markers including CD19 and Mac1. (C) Rag1/GFP$^-$ cells sorted

from E10.5 YS were stained in the same manner as for the E10.5 AGM cells described above. The profile of Tie2 and c-kit expression is shown in the upper panel. In a lower panel, ESAM expression in the $Tie2^{Hi}$ $c\text{-}kit^{Lo}$ fraction (tinted histogram) and the $Tie2^{Lo}$ $c\text{-}kit^{Hi}$ fraction (open histogram) are shown. A dashed line shows the background fluorescence with an isotype matched IgG. (D) ESAM expression of $Rag1/GFP^-$ Lin^- $ckit^{Hi}$ $Sca1^+$ cells of adult bone marrow of 3, 6, 12, and 18 months old mice were analyzed. Representative flow cytometry results in three to five mice of each age were shown. ESAM expression on $Rag1/GFP^-$ Lin^- $c\text{-}kit^{Hi}$ $Sca1^+$ cells of adult bone marrow of 3, 12, and 18 months old mice (n=3 in each) were simultaneously analyzed and the data were summarized with respect to the mean fluorescence intensity with an anti-ESAM Ab or its control Ab (right panel). (E) $ESAM^{-/Lo}$ or $ESAM^{Hi}$ cells were sorted from the $Rag1/GFP^-$ Lin^- $ckit^{Hi}$ $Sca1^+$ fraction of the indicated adult bone marrow (7 and 20 months old, respectively), and subjected to methylcellulose colony assay. The data are from one of two independent experiments that gave similar results. Asterisks indicate statistical significance (* $p<0.05$, ** $p<0.01$). The percentages of cells in each gate are indicated in each panel.

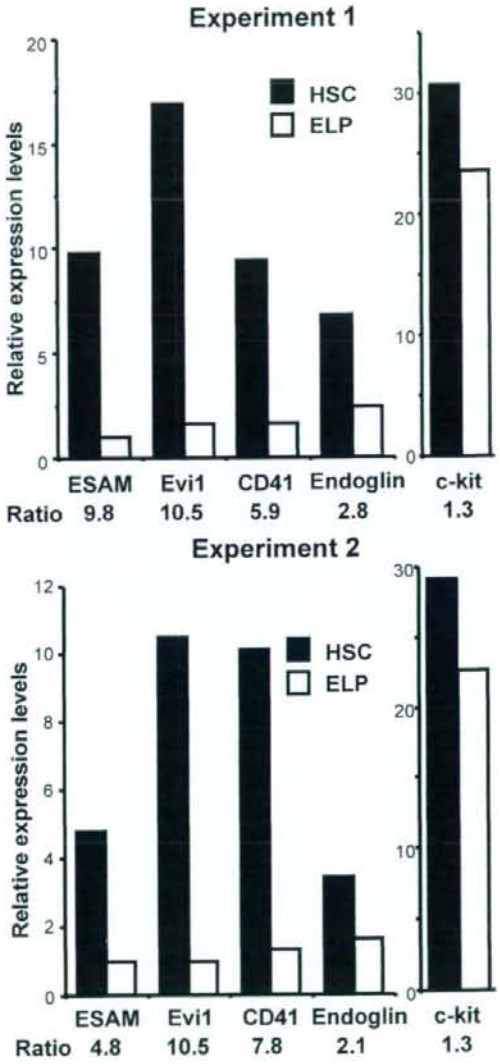
Experiment 1
Relative expression levels
HSC
ELP
ESAM
Evi1
CD41
Endoglin
c-kit
Ratio 9.8
10.5
5.9
2.8
1.3
Experiment 2
Relative expression levels
HSC
ELP
ESAM
Evi1
CD41
Endoglin
c-kit
Ratio 4.8
10.5
7.8
2.1
1.3

Figure 1

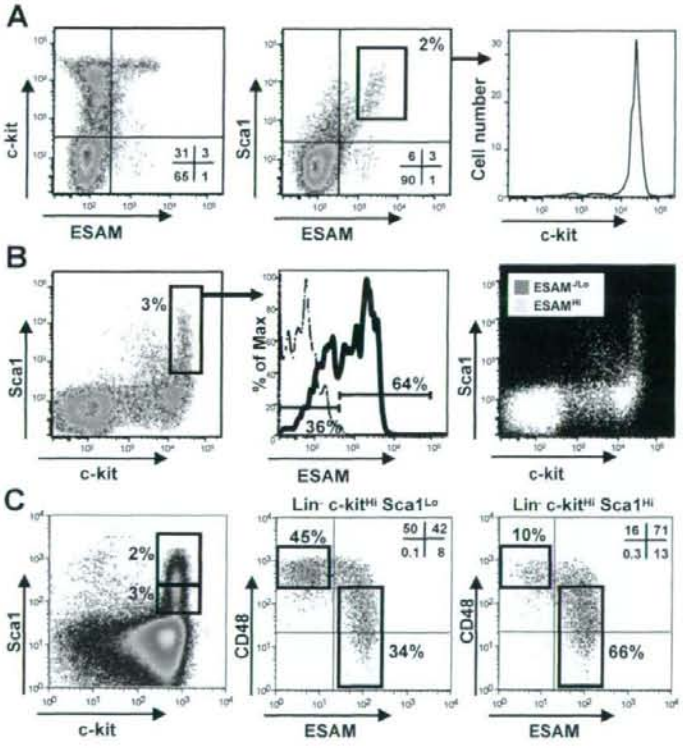
A
c-kit
ESAM
31
3
65
1
Sca1
2%
6
3
90
1
Cell number
B
Sca1
3%
c-kit
% of Max
64%
36%
ESAM
ESAM-Lo
ESAMHi
C
Lin- c-kitHi Sca1Lo
Lin- c-kitHi Sca1Hi
2%
3%
45%
50
42
0.1
8
34%
10%
16
71
0.3
13
66%
CD48

Figure 2